Anisotropy of quark-gluon plasma inferred from high $p_\perp$ data

Stefan Stojku, Institute of Physics Belgrade

In collaboration with: Magdalena Djordjevic, Marko Djordjevic, Jussi Auvinen and Pasi Huovinen

МИНИСТАРСТВО ПРОСВЕТЕ,
НАУКЕ И ТЕХНОЛОШКОГ РАЗВОЈА

Introduction

Introduction

- Energy loss of high energy particles traversing QCD medium is an excellent probe of QGP properties.

Introduction

- Energy loss of high energy particles traversing QCD medium is an excellent probe of QGP properties.
- High energy particles:
  - Are produced only during the initial stage of QCD matter

- Energy loss of high energy particles traversing QCD medium is an excellent probe of QGP properties.

- High energy particles:
  - Are produced only during the initial stage of QCD matter
  - Significantly interact with the QCD medium

Introduction

- Energy loss of high energy particles traversing QCD medium is an excellent probe of QGP properties.
- High energy particles:
  - Are produced only during the initial stage of QCD matter
  - Significantly interact with the QCD medium
  - Perturbative calculations are possible

Introduction

- Energy loss of high energy particles traversing QCD medium is an excellent probe of QGP properties.
- High energy particles:
  - Are produced only during the initial stage of QCD matter
  - Significantly interact with the QCD medium
  - Perturbative calculations are possible
- Theoretical predictions vs. experimental data.

- Energy loss of high energy particles traversing QCD medium is an excellent probe of QGP properties.
- High energy particles:
  - Are produced only during the initial stage of QCD matter
  - Significantly interact with the QCD medium
  - Perturbative calculations are possible
- Theoretical predictions vs. experimental data.
- DREENA framework: a versatile and fully optimized suppression calculation procedure (talk by Magdalena Djordjevic).

- Dynamical Radiative and Elastic ENergy Loss Approach

Introduction

- Dynamical Radiative and Elastic ENergy Loss Approach
- Capable of generating high-$p_{\perp}$ predictions for:
  - different collision systems
  - collision energies
  - centralities
  - observables...
- Versions: DREENA-C, DREENA-B, DREENA-A

- Next goal: use high-$p_\perp$ data to infer bulk properties of QGP.

- Next goal: use high-$p_\perp$ data to infer bulk properties of QGP.

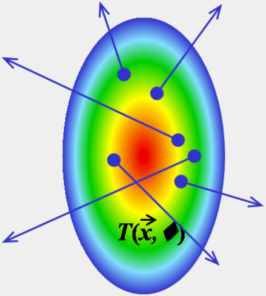

- High energy particles lose energy when they traverse QGP.

QGP TOMOGRAPHY

- Next goal: use high-$p_\perp$ data to infer bulk properties of QGP.

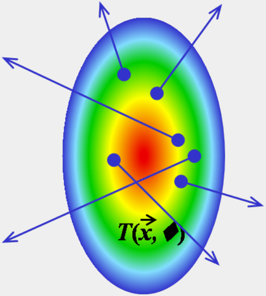

- High energy particles lose energy when they traverse QGP.
- This energy loss is sensitive to QGP properties.

QGP TOMOGRAPHY

- Next goal: use high-$p_\perp$ data to infer bulk properties of QGP.

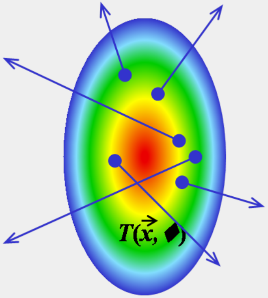

- High energy particles lose energy when they traverse QGP.
- This energy loss is sensitive to QGP properties.
- We can realistically predict this energy loss.

- Next goal: use high-$p_\perp$ data to infer bulk properties of QGP.

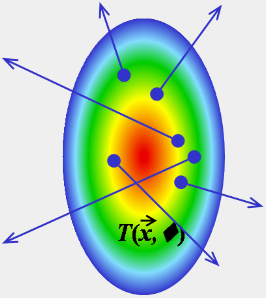

- High energy particles lose energy when they traverse QGP.
- This energy loss is sensitive to QGP properties.
- We can realistically predict this energy loss.

- High-$p_\perp$ probes are excellent tomoraphy tools.
- We can use them to infer some of the bulk QGP properties.

How to infer the shape of the QGP droplet from the data?

Shape of the QGP droplet

- Initial spatial anisotropy is one of the main properties of QGP.
- A major limiting factor for QGP tomography.

- Initial spatial anisotropy is one of the main properties of QGP.
- A major limiting factor for QGP tomography.
- Still not possible to directly infer the initial anisotropy from experimental data.

- Initial spatial anisotropy is one of the main properties of QGP.
- A major limiting factor for QGP tomography.
- Still not possible to directly infer the initial anisotropy from experimental data.
- Several theoretical studies (MC-Glauber, EKRT, IP-Glasma, MC-KLN) infer the initial anisotropy; lead to notably different predictions.

Shape of the QGP droplet

- Initial spatial anisotropy is one of the main properties of QGP.
- A major limiting factor for QGP tomography.
- Still not possible to directly infer the initial anisotropy from experimental data.
- Several theoretical studies (MC-Glauber, EKRT, IP-Glasma, MC-KLN) infer the initial anisotropy; lead to notably different predictions.

⬇

- Alternative approaches for inferring anisotropy are necessary!

Shape of the QGP droplet

- Initial spatial anisotropy is one of the main properties of QGP.
- A major limiting factor for QGP tomography.
- Still not possible to directly infer the initial anisotropy from experimental data.
- Several theoretical studies (MC-Glauber, EKRT, IP-Glasma, MC-KLN) infer the initial anisotropy; lead to notably different predictions.

⬇

- Alternative approaches for inferring anisotropy are necessary!
- Optimally, these should be complementary to existing predictions.

Shape of the QGP droplet

- Initial spatial anisotropy is one of the main properties of QGP.
- A major limiting factor for QGP tomography.
- Still not possible to directly infer the initial anisotropy from experimental data.
- Several theoretical studies (MC-Glauber, EKRT, IP-Glasma, MC-KLN) infer the initial anisotropy; lead to notably different predictions.

⬇

- Alternative approaches for inferring anisotropy are necessary!
- Optimally, these should be complementary to existing predictions.
- Based on a method that is fundamentally different than models of early stages of QCD matter.

- Inference from already available high-$p_\perp$ R_{AA} and v_2 measurements (to be measured with higher precision in the future).

- Inference from already available high-$p_\perp$ R_{AA} and v_2 measurements (to be measured with higher precision in the future).
- Use experimental data (rather than calculations which rely on early stages of QCD matter).
- Exploit information from interactions of rare high-$p_\perp$ partons with QCD medium.

- Inference from already available high-$p_\perp$ R_{AA} and v_2 measurements (to be measured with higher precision in the future).

- Use experimental data (rather than calculations which rely on early stages of QCD matter).
- Exploit information from interactions of rare high-$p_\perp$ partons with QCD medium.

- Advances the applicability of high-$p_\perp$ data.
- Up to now, this data was mainly used to study the jet-medium interactions, rather than inferring bulk QGP parameters.

What is an appropriate observable?

The initial state anisotropy is quantified in terms of eccentricity parameter ϵ_2:

$$\epsilon_2 = \frac{\langle y^2 - x^2 \rangle}{\langle y^2 + x^2 \rangle} = \frac{\int dx\, dy\, (y^2 - x^2)\, \rho(x, y)}{\int dx\, dy\, (y^2 + x^2)\, \rho(x, y)},$$

where $\rho(x, y)$ is the initial density distribution of the QGP droplet.

M. Djordjevic, S. Stojku, M. Djordjevic and P. Huovinen, Phys.Rev. C Rapid Commun. 100, 031901 (2019).

What is an appropriate observable?

The initial state anisotropy is quantified in terms of eccentricity parameter ϵ_2:

$$\epsilon_2 = \frac{\langle y^2 - x^2 \rangle}{\langle y^2 + x^2 \rangle} = \frac{\int dx\, dy\, (y^2 - x^2)\, \rho(x, y)}{\int dx\, dy\, (y^2 + x^2)\, \rho(x, y)},$$

where $\rho(x, y)$ is the initial density distribution of the QGP droplet.

M. Djordjevic, S. Stojku, M. Djordjevic and P. Huovinen, Phys.Rev. C Rapid Commun. 100, 031901 (2019).

- High-$p_\perp$ v_2 is sensitive to both the anisotropy and the size of the system.
- R_{AA} is sensitive only to the size of the system.

What is an appropriate observable?

The initial state anisotropy is quantified in terms of eccentricity parameter ϵ_2:

$$\epsilon_2 = \frac{\langle y^2 - x^2 \rangle}{\langle y^2 + x^2 \rangle} = \frac{\int dx\, dy\, (y^2 - x^2)\, \rho(x,y)}{\int dx\, dy\, (y^2 + x^2)\, \rho(x,y)},$$

where $\rho(x, y)$ is the initial density distribution of the QGP droplet.

M. Djordjevic, S. Stojku, M. Djordjevic and P. Huovinen, Phys.Rev. C Rapid Commun. 100, 031901 (2019).

- High-$p_\perp$ v_2 is sensitive to both the anisotropy and the size of the system.
- R_{AA} is sensitive only to the size of the system.

⬇

Can we extract eccentricity from high-$p_\perp$ R_{AA} and v_2?

Anisotropy observable

Use scaling arguments for high-$p_\perp$

$\Delta E/E \approx \langle T \rangle^a \langle L \rangle^b$, where within our model $a \approx 1.2$, $b \approx 1.4$

D. Zigic *et al.*, JPG 46, 085101 (2019); M. Djordjevic and M. Djordjevic, PRC 92, 024918 (2015)

Use scaling arguments for high-$p_\perp$

$\Delta E/E \approx \langle T\rangle^a \langle L\rangle^b$, where within our model $a \approx 1.2$, $b \approx 1.4$

D. Zigic *et al.*, JPG 46, 085101 (2019); M. Djordjevic and M. Djordjevic, PRC 92, 024918 (2015)

$$R_{AA} \approx 1 - \xi \langle T\rangle^a \langle L\rangle^b$$

$$1 - R_{AA} \approx \xi \langle T\rangle^a \langle L\rangle^b$$

$$v_2 \approx \frac{1}{2}\frac{R_{AA}^{in} - R_{AA}^{out}}{R_{AA}^{in} + R_{AA}^{out}} \Longrightarrow$$

$$v_2 \approx \xi \langle T\rangle^a \langle L\rangle^b \left(\frac{b}{2}\frac{\Delta L}{\langle L\rangle} - \frac{a}{2}\frac{\Delta T}{\langle T\rangle}\right)$$

Anisotropy observable

Use scaling arguments for high-$p_\perp$

$\Delta E/E \approx \langle T\rangle^a \langle L\rangle^b$, where within our model $a \approx 1.2$, $b \approx 1.4$

D. Zigic *et al.*, JPG 46, 085101 (2019); M. Djordjevic and M. Djordjevic, PRC 92, 024918 (2015)

$$R_{AA} \approx 1 - \xi \langle T\rangle^a \langle L\rangle^b$$

$$1 - R_{AA} \approx \xi \langle T\rangle^a \langle L\rangle^b$$

$$v_2 \approx \frac{1}{2}\frac{R_{AA}^{in} - R_{AA}^{out}}{R_{AA}^{in} + R_{AA}^{out}} \Longrightarrow$$

$$v_2 \approx \xi \langle T\rangle^a \langle L\rangle^b \left(\frac{b}{2}\frac{\Delta L}{\langle L\rangle} - \frac{a}{2}\frac{\Delta T}{\langle T\rangle}\right)$$

⬇

$$\boxed{\frac{v_2}{1 - R_{AA}} \approx \left(\frac{b}{2}\frac{\Delta L}{\langle L\rangle} - \frac{a}{2}\frac{\Delta T}{\langle T\rangle}\right)}$$

This ratio carries information on the asymmetry of the system, but through both spatial and temperature variables.

M. Djordjevic, S. Stojku, M. Djordjevic and P. Huovinen, Phys.Rev. C Rapid Commun. 100, 031901 (2019).

Anisotropy parameter ς

Temperature vs. spatial asymmetry:

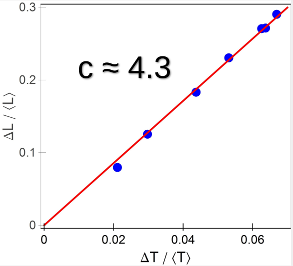

$$\frac{v_2}{1 - R_{AA}} \approx \left(\frac{b}{2} \frac{\Delta L}{\langle L \rangle} - \frac{a}{2} \frac{\Delta T}{\langle T \rangle} \right) \implies$$

ANISOTROPY PARAMETER ς

Temperature vs. spatial asymmetry:

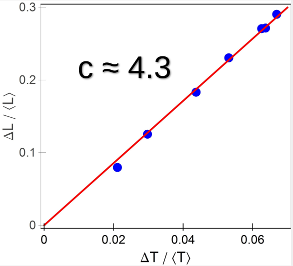

$$\frac{v_2}{1-R_{AA}} \approx \left(\frac{b}{2}\frac{\Delta L}{\langle L\rangle} - \frac{a}{2}\frac{\Delta T}{\langle T\rangle}\right) \Longrightarrow$$

$$\frac{v_2}{1-R_{AA}} \approx \frac{1}{2}\left(b - \frac{a}{c}\right)\frac{\langle L_{out}\rangle - \langle L_{in}\rangle}{\langle L_{out}\rangle + \langle L_{in}\rangle} \approx 0.57\varsigma$$

$$\varsigma = \frac{\Delta L}{\langle L\rangle} = \frac{\langle L_{out}\rangle - \langle L_{in}\rangle}{\langle L_{out}\rangle + \langle L_{in}\rangle}$$

Anisotropy parameter ς

Temperature vs. spatial asymmetry:

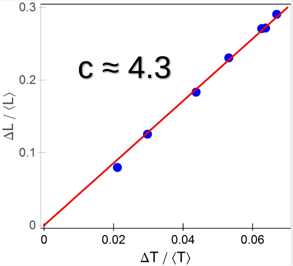

$$\frac{v_2}{1-R_{AA}} \approx \left(\frac{b}{2}\frac{\Delta L}{\langle L\rangle} - \frac{a}{2}\frac{\Delta T}{\langle T\rangle}\right) \Longrightarrow$$

$$\boxed{\frac{v_2}{1-R_{AA}} \approx \frac{1}{2}\left(b-\frac{a}{c}\right)\frac{\langle L_{out}\rangle - \langle L_{in}\rangle}{\langle L_{out}\rangle + \langle L_{in}\rangle} \approx 0.57\varsigma}$$

$$\boxed{\varsigma = \frac{\Delta L}{\langle L\rangle} = \frac{\langle L_{out}\rangle - \langle L_{in}\rangle}{\langle L_{out}\rangle + \langle L_{in}\rangle}}$$

- At high $p_\perp$, v_2 over $1-R_{AA}$ ratio is dictated *solely* by the geometry of the initial fireball!
- Anisotropy parameter ς follows directly from high $p_\perp$ experimental data!

M. Djordjevic, S. Stojku, M. Djordjevic and P. Huovinen, Phys.Rev. C Rapid Commun. 100, 031901 (2019).

DREENA-B results vs. experimental data

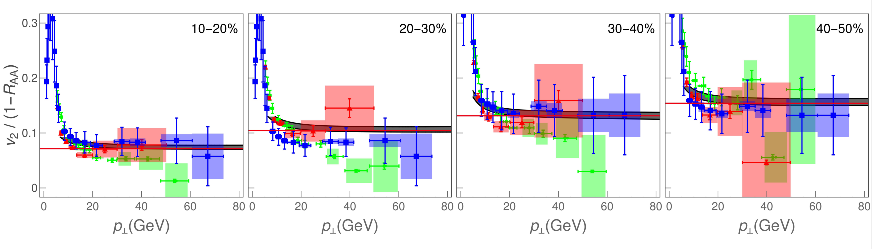

- Solid red line: analytically derived asymptote.

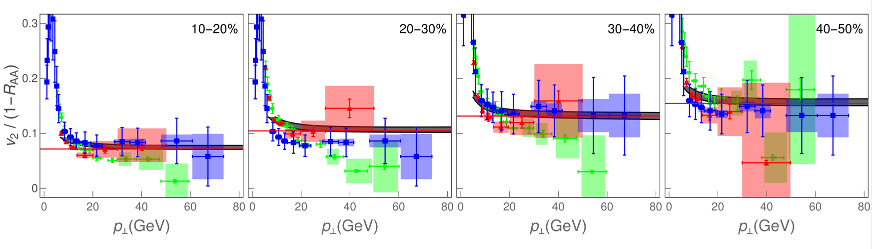

- Solid red line: analytically derived asymptote.
- For each centrality and from $p_\perp \approx 20 GeV$, $v_2/(1-R_{AA})$ does not depend on $p_\perp$, but is determined by the geometry of the system.

DREENA-B RESULTS VS. EXPERIMENTAL DATA

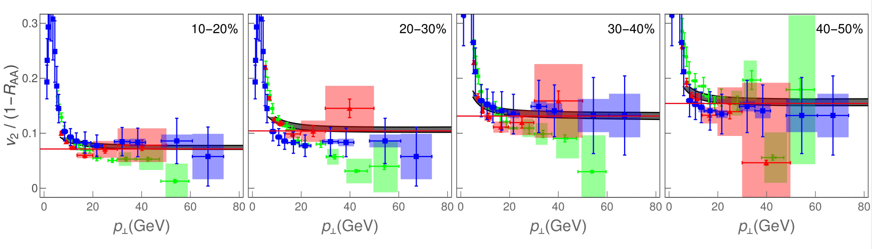

- Solid red line: analytically derived asymptote.
- For each centrality and from $p_\perp \approx 20 GeV$, $v_2/(1-R_{AA})$ does not depend on $p_\perp$, but is determined by the geometry of the system.
- The experimental data from ALICE, CMS and ATLAS show the same tendency, though the error bars are still large.
- In the LHC Run 3 the error bars should be significantly reduced.

Comparison with experimental data

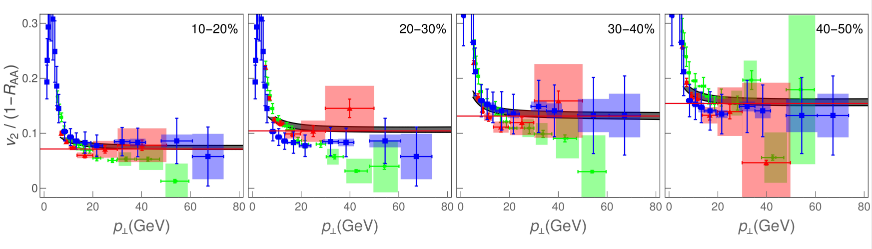

- $v_2/(1-R_{AA})$ indeed carries the information about the system's anisotropy.
- It can be simply (from the straight line high-$p_\perp$ limit) and robustly (in the same way for each centrality) inferred from experimental data.

Anisotropy parameter ς is not the commonly used anisotropy parameter ϵ_2. To facilitate comparison with ϵ_2 values in the literature, we define:

$$\epsilon_{2L} = \frac{\langle L_{out} \rangle^2 - \langle L_{in} \rangle^2}{\langle L_{out} \rangle^2 + \langle L_{in} \rangle^2} = \frac{2\varsigma}{1+\varsigma^2} \implies$$

M. Djordjevic, S. Stojku, M. Djordjevic and P. Huovinen, Phys.Rev. C Rapid Commun. 100, 031901 (2019).

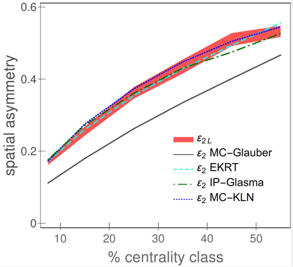

Eccentricity

Anisotropy parameter ς is not the commonly used anisotropy parameter ϵ_2. To facilitate comparison with ϵ_2 values in the literature, we define:

$$\epsilon_{2L} = \frac{\langle L_{out} \rangle^2 - \langle L_{in} \rangle^2}{\langle L_{out} \rangle^2 + \langle L_{in} \rangle^2} = \frac{2\varsigma}{1+\varsigma^2} \implies$$

M. Djordjevic, S. Stojku, M. Djordjevic and P. Huovinen, Phys.Rev. C Rapid Commun. 100, 031901 (2019).

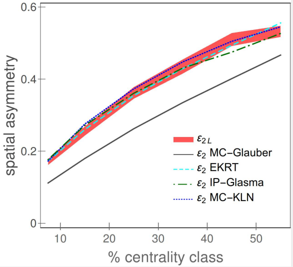

ϵ_{2L} is in an excellent agreement with ϵ_2 which we started from.

⬇

$v_2/(1-R_{AA})$ provides a reliable and robust procedure to recover initial state anisotropy.

Anisotropy parameter ς is not the commonly used anisotropy parameter ϵ_2. To facilitate comparison with ϵ_2 values in the literature, we define:

$$\epsilon_{2L} = \frac{\langle L_{out}\rangle^2 - \langle L_{in}\rangle^2}{\langle L_{out}\rangle^2 + \langle L_{in}\rangle^2} = \frac{2\varsigma}{1+\varsigma^2} \Longrightarrow$$

M. Djordjevic, S. Stojku, M. Djordjevic and P. Huovinen, Phys.Rev. C Rapid Commun. 100, 031901 (2019).

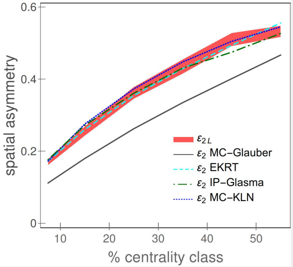

ϵ_{2L} is in an excellent agreement with ϵ_2 which we started from.

$v_2/(1-R_{AA})$ provides a reliable and robust procedure to recover initial state anisotropy.

The width of our ϵ_{2L} band is smaller than the difference in ϵ_2 values obtained by using different models.

Resolving power to distinguish between different initial state models

What happens when we include full medium evolution?

DREENA-A

- Full medium evolution $\Longrightarrow$ DREENA-A

  D. Zigic, I. Salom, J. Auvinen, P. Huovinen and M. Djordjevic, arXiv:2110.01544 [nucl-th].

- "A" - adaptive

DREENA-A

- Full medium evolution $\Longrightarrow$ DREENA-A

  D. Zigic, I. Salom, J. Auvinen, P. Huovinen and M. Djordjevic, arXiv:2110.01544 [nucl-th].

- "A" - adaptive
- Most up-to-date version of our framework

DREENA-A

- Full medium evolution $\Longrightarrow$ DREENA-A

  D. Zigic, I. Salom, J. Auvinen, P. Huovinen and M. Djordjevic, arXiv:2110.01544 [nucl-th].

- "A" - adaptive
- Most up-to-date version of our framework
- It can accommodate any QGP temperature profile and generate R_{AA} and v_2 predictions
- ...which can be directly compared with the experimental results.

DREENA-A

- Full medium evolution $\Longrightarrow$ DREENA-A

  D. Zigic, I. Salom, J. Auvinen, P. Huovinen and M. Djordjevic, arXiv:2110.01544 [nucl-th].

- "A" - adaptive
- Most up-to-date version of our framework
- It can accommodate any QGP temperature profile and generate R_{AA} and v_2 predictions
- ...which can be directly compared with the experimental results.
- It retains all the features of our state-of-the-art energy loss model.

DREENA-A

- Full medium evolution $\Longrightarrow$ DREENA-A

  D. Zigic, I. Salom, J. Auvinen, P. Huovinen and M. Djordjevic, arXiv:2110.01544 [nucl-th].

- "A" - adaptive
- Most up-to-date version of our framework
- It can accommodate any QGP temperature profile and generate R_{AA} and v_2 predictions
- ...which can be directly compared with the experimental results.
- It retains all the features of our state-of-the-art energy loss model.

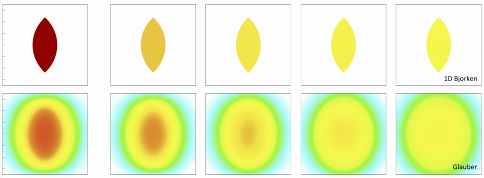

Figure adapted from D. Zigic, I. Salom, J. Auvinen, P. Huovinen and M. Djordjevic, arXiv:2110.01544 [nucl-th].

DREENA-A

- Collision system - locally thermalized dissipative fluid.

DREENA-A

- Collision system - locally thermalized dissipative fluid.
- We test various different initializations of fluid-dynamical evolution.

DREENA-A

- Collision system - locally thermalized dissipative fluid.
- We test various different initializations of fluid-dynamical evolution.
- To provide physical results, one must use temperature profiles that reproduce low-$p_\perp$ results.

DREENA-A

- Collision system - locally thermalized dissipative fluid.
- We test various different initializations of fluid-dynamical evolution.
- To provide physical results, one must use temperature profiles that reproduce low-$p_\perp$ results.
- Glauber, EKRT, TRENTO, IP-Glasma

DREENA-A

- Collision system - locally thermalized dissipative fluid.
- We test various different initializations of fluid-dynamical evolution.
- To provide physical results, one must use temperature profiles that reproduce low-$p_\perp$ results.
- Glauber, EKRT, TRENTO, IP-Glasma
- Various QGP simulations evolve differently, $v_2/(1-R_{AA})$ relates to the average anisotropy of the system.
- Define a suitable anisotropy observable?

DREENA-A

- We visualize the temperatures partons experience...

DREENA-A

- We visualize the temperatures partons experience...
- ... in the in-plane and out-of-plane directions.

Stefan Stojku, Jussi Auvinen, Pasi Huovinen, Magdalena Djordjevic, arXiv:2110.02029[nucl-th]

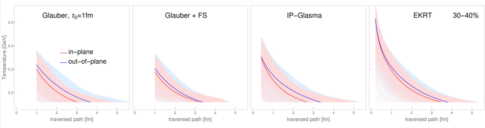

$$\langle T_x(t)\rangle = \frac{1}{N}\sum_{i=1}^{N} T(x_i + t, y_i, t)$$

$$\langle T_y(t)\rangle = \frac{1}{N}\sum_{i=1}^{N} T(x_i, y_i + t, t)$$

- larger $T \implies$ larger suppression
- larger $T_{out} - T_{in} \implies$ larger v_2
- The medium affects partons in the in-plane and out-of-plane directions differently

DREENA-A

- We visualize the temperatures partons experience...
- ... in the in-plane and out-of-plane directions.

Stefan Stojku, Jussi Auvinen, Pasi Huovinen, Magdalena Djordjevic, arXiv:2110.02029[nucl-th]

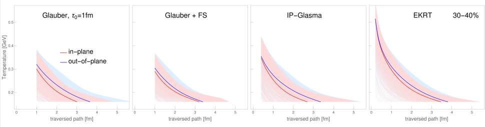

$$\langle T_x(t)\rangle = \frac{1}{N}\sum_{i=1}^{N} T(x_i + t, y_i, t)$$

$$\langle T_y(t)\rangle = \frac{1}{N}\sum_{i=1}^{N} T(x_i, y_i + t, t)$$

1. Does $v_2/(1 - R_{AA})$ saturate?

DREENA-A

- We visualize the temperatures partons experience...
- ... in the in-plane and out-of-plane directions.

Stefan Stojku, Jussi Auvinen, Pasi Huovinen, Magdalena Djordjevic, arXiv:2110.02029[nucl-th]

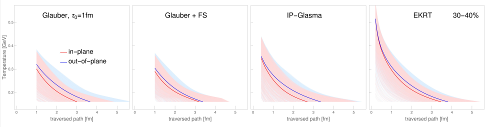

$$\langle T_x(t) \rangle = \frac{1}{N} \sum_{i=1}^{N} T(x_i + t, y_i, t)$$

$$\langle T_y(t) \rangle = \frac{1}{N} \sum_{i=1}^{N} T(x_i, y_i + t, t)$$

1. Does $v_2/(1 - R_{AA})$ saturate?
2. Does this saturation carry information on the anisotropy of the system?

DREENA-A

- We visualize the temperatures partons experience...
- ... in the in-plane and out-of-plane directions.

Stefan Stojku, Jussi Auvinen, Pasi Huovinen, Magdalena Djordjevic, arXiv:2110.02029[nucl-th]

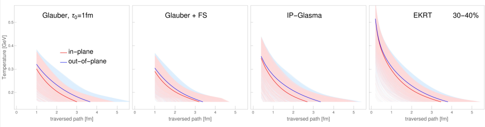

$$\langle T_x(t)\rangle = \frac{1}{N}\sum_{i=1}^{N} T(x_i + t, y_i, t)$$

$$\langle T_y(t)\rangle = \frac{1}{N}\sum_{i=1}^{N} T(x_i, y_i + t, t)$$

1. Does $v_2/(1-R_{AA})$ saturate?
2. Does this saturation carry information on the anisotropy of the system?
3. What kind of anisotropy measure is revealed through high-$p_\perp$ data?

- Next: we show $v_2/(1-R_{AA})$ results for various temperature profiles

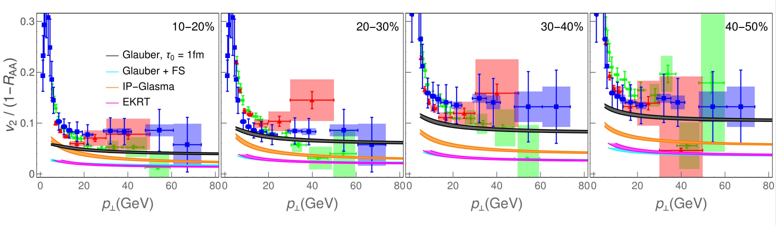

Stefan Stojku, Jussi Auvinen, Pasi Huovinen, Magdalena Djordjevic, arXiv:2110.02029[nucl-th]

DREENA-A RESULTS

- Next: we show $v_2/(1-R_{AA})$ results for various temperature profiles

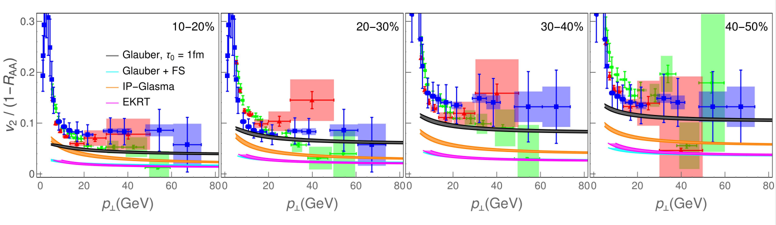

Stefan Stojku, Jussi Auvinen, Pasi Huovinen, Magdalena Djordjevic, arXiv:2110.02029[nucl-th]

- $v_2/(1-R_{AA})$ reaches a constant value above $p_\perp = 30GeV$ for all profiles.

DREENA-A RESULTS

- Next: we show $v_2/(1-R_{AA})$ results for various temperature profiles

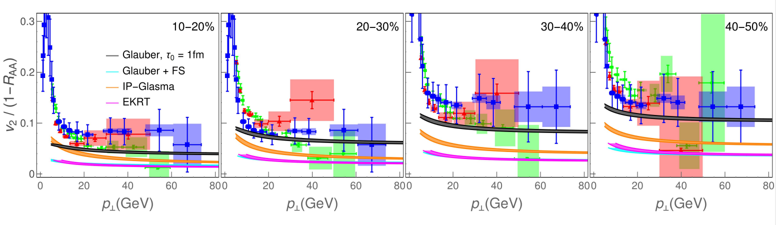

Stefan Stojku, Jussi Auvinen, Pasi Huovinen, Magdalena Djordjevic, arXiv:2110.02029[nucl-th]

- $v_2/(1-R_{AA})$ reaches a constant value above $p_\perp = 30 GeV$ for all profiles.
- Thus, the phenomenon of $v_2/(1-R_{AA})$ saturation is robust.

- How to explore if this $v_2/(1 - R_{AA})$ contains information on the system anisotropy?

Connection to anisotropy

- How to explore if this $v_2/(1-R_{AA})$ contains information on the system anisotropy?
- DREENA-A: dynamical tracking using Monte Carlo-generated trajectories.

$$\frac{\Delta L}{\langle L \rangle} = \frac{\langle L_{out} \rangle - \langle L_{in} \rangle}{\langle L_{out} \rangle + \langle L_{in} \rangle}$$

Connection to anisotropy

- How to explore if this $v_2/(1 - R_{AA})$ contains information on the system anisotropy?
- DREENA-A: dynamical tracking using Monte Carlo-generated trajectories.

$$\frac{\Delta L}{\langle L \rangle} = \frac{\langle L_{out} \rangle - \langle L_{in} \rangle}{\langle L_{out} \rangle + \langle L_{in} \rangle}$$

- We evaluate $\Delta L/\langle L \rangle$:

- How to explore if this $v_2/(1 - R_{AA})$ contains information on the system anisotropy?
- DREENA-A: dynamical tracking using Monte Carlo-generated trajectories.

$$\frac{\Delta L}{\langle L \rangle} = \frac{\langle L_{out} \rangle - \langle L_{in} \rangle}{\langle L_{out} \rangle + \langle L_{in} \rangle}$$

- We evaluate $\Delta L / \langle L \rangle$:
    1. Generate a hard parton in the XY plane according to binary collision densities.

Connection to anisotropy

- How to explore if this $v_2/(1 - R_{AA})$ contains information on the system anisotropy?
- DREENA-A: dynamical tracking using Monte Carlo-generated trajectories.

$$\frac{\Delta L}{\langle L \rangle} = \frac{\langle L_{out} \rangle - \langle L_{in} \rangle}{\langle L_{out} \rangle + \langle L_{in} \rangle}$$

- We evaluate $\Delta L / \langle L \rangle$:
  1. Generate a hard parton in the XY plane according to binary collision densities.
  2. The parton traverses the medium in the $\phi = 0$ (or $\phi = \pi/2$) direction, until $T_{local} < T_c$.

- How to explore if this $v_2/(1 - R_{AA})$ contains information on the system anisotropy?
- DREENA-A: dynamical tracking using Monte Carlo-generated trajectories.

$$\frac{\Delta L}{\langle L \rangle} = \frac{\langle L_{out} \rangle - \langle L_{in} \rangle}{\langle L_{out} \rangle + \langle L_{in} \rangle}$$

- We evaluate $\Delta L/\langle L \rangle$:
  1. Generate a hard parton in the XY plane according to binary collision densities.
  2. The parton traverses the medium in the $\phi = 0$ (or $\phi = \pi/2$) direction, until $T_{local} < T_c$.
  3. Obtain $\langle L_{in} \rangle$ (and $\langle L_{out} \rangle$) by averaging over trajectories of many partons.

Connection to anisotropy

- **Next:** Plot charged hadrons' $v_2/(1 - R_{AA})[100GeV]$ vs. $\Delta L/\langle L \rangle$

  Stefan Stojku, Jussi Auvinen, Pasi Huovinen, Magdalena Djordjevic, arXiv:2110.02029[nucl-th]

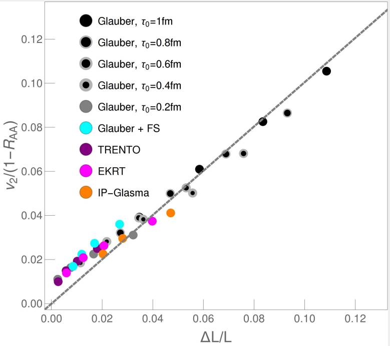

- Centrality classes: 10-20%, 20-30%, 30-40%, 40-50%

- **Next:** Plot charged hadrons' $v_2/(1-R_{AA})[100GeV]$ vs. $\Delta L/\langle L\rangle$

Stefan Stojku, Jussi Auvinen, Pasi Huovinen, Magdalena Djordjevic, arXiv:2110.02029[nucl-th]

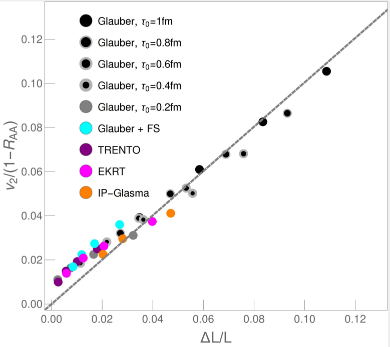

- Centrality classes: 10-20%, 20-30%, 30-40%, 40-50%
- Surprisingly simple relation between $v_2/(1-R_{AA})$ and $\Delta L/\langle L\rangle$.
- Slope $\approx$ 1.

Connection to anisotropy

- **Next:** Plot charged hadrons' $v_2/(1-R_{AA})[100GeV]$ vs. $\Delta L/\langle L\rangle$

  Stefan Stojku, Jussi Auvinen, Pasi Huovinen, Magdalena Djordjevic, arXiv:2110.02029[nucl-th]

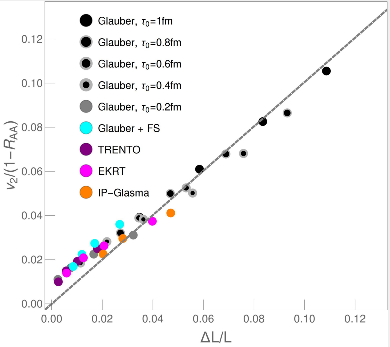

- Centrality classes: 10-20%, 20-30%, 30-40%, 40-50%
- Surprisingly simple relation between $v_2/(1-R_{AA})$ and $\Delta L/\langle L\rangle$.
- Slope $\approx$ 1.
- $v_2/(1-R_{AA})$ carries information on the system anisotropy, through $\Delta L/\langle L\rangle$.

Jet-temperature anisotropy

- $\Delta L/\langle L\rangle$

- $\Delta L / \langle L \rangle$
- A more direct measure of anisotropy?
- With an explicit dependence on time-evolution?

- $\Delta L/\langle L\rangle$
- A more direct measure of anisotropy?
- With an explicit dependence on time-evolution?
- We define jT:

$$jT(\tau,\phi) \equiv \frac{\int dxdy\, T^3(x+\tau\cos\phi, y+\tau\sin\phi,\tau)\, n_0(x,y)}{\int dxdy\, n_0(x,y)}$$

- $\Delta L/\langle L\rangle$
- A more direct measure of anisotropy?
- With an explicit dependence on time-evolution?
- We define *jT*:

$$jT(\tau,\phi) \equiv \frac{\int dxdy\, T^3(x+\tau\cos\phi, y+\tau\sin\phi, \tau)\, n_0(x,y)}{\int dxdy\, n_0(x,y)}$$

- *jT* is not azimuthally symmetric. We define its 2^{nd} Fourier coefficient jT_2:

$$jT_2(\tau) = \frac{\int dxdy\, n_0(x,y) \int \phi \cos 2\phi\, T^3(x+\tau\cos\phi, y+\tau\sin\phi, \tau)}{\int dxdy\, n_0(x,y) \int \phi\, T^3(x+\tau\cos\phi, y+\tau\sin\phi, \tau)}$$

- We then define a simple time average of jT_2:

$$\langle jT_2 \rangle = \frac{\int_{\tau_0}^{\tau_{\rm cut}} d\tau \, jT_2(\tau)}{\tau_{\rm cut} - \tau_0}$$

Stefan Stojku, Jussi Auvinen, Pasi Huovinen, Magdalena Djordjevic, arXiv:2110.02029[nucl-th]

- We then define a simple time average of jT_2:

$$\langle jT_2 \rangle = \frac{\int_{\tau_0}^{\tau_{\rm cut}} d\tau\, jT_2(\tau)}{\tau_{\rm cut} - \tau_0}$$

Stefan Stojku, Jussi Auvinen, Pasi Huovinen, Magdalena Djordjevic, arXiv:2110.02029[nucl-th]

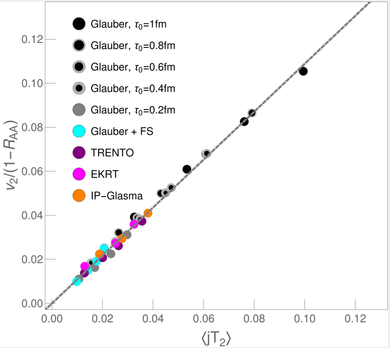

- We then define a simple time average of jT_2:

$$\langle jT_2 \rangle = \frac{\int_{\tau_0}^{\tau_{\rm cut}} d\tau \, jT_2(\tau)}{\tau_{\rm cut} - \tau_0}$$

Stefan Stojku, Jussi Auvinen, Pasi Huovinen, Magdalena Djordjevic, arXiv:2110.02029[nucl-th]

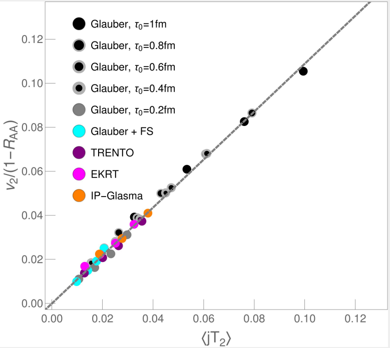

- $v2/(1 - R_{AA})$ shows a linear dependence on $\langle jT_2 \rangle$, with a slope close to 1.

Jet-temperature anisotropy

- We then define a simple time average of jT_2:

$$\langle jT_2 \rangle = \frac{\int_{\tau_0}^{\tau_{\rm cut}} d\tau \, jT_2(\tau)}{\tau_{\rm cut} - \tau_0}$$

Stefan Stojku, Jussi Auvinen, Pasi Huovinen, Magdalena Djordjevic, arXiv:2110.02029[nucl-th]

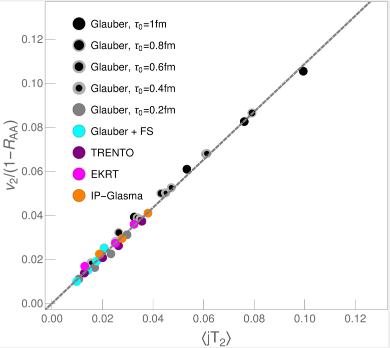

- $v2/(1-R_{AA})$ shows a linear dependence on $\langle jT_2 \rangle$, with a slope close to 1.
- Therefore, $v_2/(1-R_{AA})$ carries information on this property of the medium.

Summary

- High-$p_{\perp}$ theory and data - traditionally used to explore high-$p_{\perp}$ parton interactions with QGP.

Summary

- High-$p_\perp$ theory and data - traditionally used to explore high-$p_\perp$ parton interactions with QGP.
- High-$p_\perp$ probes can become powerful tomography tools, as they are sensitive to global QGP properties (e.g. spatial anisotropy).

Summary

- High-$p_\perp$ theory and data - traditionally used to explore high-$p_\perp$ parton interactions with QGP.
- High-$p_\perp$ probes can become powerful tomography tools, as they are sensitive to global QGP properties (e.g. spatial anisotropy).
- A (modified) ratio of R_{AA} and v_2 - a reliable and robust observable for straightforward extraction of spatial anisotropy.

Summary

- High-$p_\perp$ theory and data - traditionally used to explore high-$p_\perp$ parton interactions with QGP.
- High-$p_\perp$ probes can become powerful tomography tools, as they are sensitive to global QGP properties (e.g. spatial anisotropy).
- A (modified) ratio of R_{AA} and v_2 - a reliable and robust observable for straightforward extraction of spatial anisotropy.
- The saturation is directly proportional to jet-temperature anisotropy.

Summary

- High-$p_\perp$ theory and data - traditionally used to explore high-$p_\perp$ parton interactions with QGP.
- High-$p_\perp$ probes can become powerful tomography tools, as they are sensitive to global QGP properties (e.g. spatial anisotropy).
- A (modified) ratio of R_{AA} and v_2 - a reliable and robust observable for straightforward extraction of spatial anisotropy.
- The saturation is directly proportional to jet-temperature anisotropy.
- It will be possible to infer anisotropy directly from LHC Run 3 data: an important constraint to models describing the early stages of QGP formation.

Summary

- High-$p_\perp$ theory and data - traditionally used to explore high-$p_\perp$ parton interactions with QGP.
- High-$p_\perp$ probes can become powerful tomography tools, as they are sensitive to global QGP properties (e.g. spatial anisotropy).
- A (modified) ratio of R_{AA} and v_2 - a reliable and robust observable for straightforward extraction of spatial anisotropy.
- The saturation is directly proportional to jet-temperature anisotropy.
- It will be possible to infer anisotropy directly from LHC Run 3 data: an important constraint to models describing the early stages of QGP formation.
- Synergy of more common approaches for inferring QGP properties with high-$p_\perp$ theory and data.

Acknowledgements

European Research Council

Established by the European Commission

МИНИСТАРСТВО ПРОСВЕТЕ,
НАУКЕ И ТЕХНОЛОШКОГ РАЗВОЈА

The speaker has received funding from the European Research Council (ERC) under the European Union’s Horizon 2020 research and innovation programme (grant agreement No 725741)

Backup

Our starting point and reference is a simple optical Glauber model based initialization, which we use at different initial times $\tau_0 = 0.2$, 0.4, 0.6, 0.8 and 1.0 fm. The initialization and code used to solve viscous fluid-dynamical equations in 3+1 dimensions are described in detail in Ref. [10], and parameters to describe Pb+Pb collisions at $\sqrt{s_{\mathrm{NN}}} = 5.02$ TeV at Ref. [11]. In particular, we use a constant shear viscosity to entropy density ratio $\eta/s = 0.12$, and the EoS parametrization $s95p$-PCE-v1 [13].

Our second option, Glauber + Free streaming, is to use the Glauber model to provide the initial distribution of (marker) particles, allow the particles to stream freely from $\tau = 0.2$ to 1.0 fm, evaluate the energy-momentum tensor of these particles, and use it as the initial state of the fluid. We evolve the fluid using the same code as in the case of pure Glauber initialization. The EoS is $s95p$-PCE175, i.e., a parametrization with $T_{\mathrm{chem}} = 175$ MeV [14], and temperature-independent $\eta/s = 0.16$. For further details, see Ref. [11].

As more sophisticated initializations, we employ EKRT, IP-Glasma and $\mathrm{T_R ENTo}$. The EKRT model [15–17] is based on the NLO perturbative QCD computation of the transverse energy and a gluon saturation conjecture. We employ the same setup as used in Ref. [18] (see also [14]), compute an ensemble of event-by-event fluctuating initial density distributions, average them, and use this average as the initial state of the fluid dynamical evolution. We again use the code of Molnar et al., [10], but restricted to boost-invariant expansion. The shear viscosity over entropy density ratio is temperature dependent with favored parameter values from the Bayesian analysis of Ref. [18]. Initial time is $\tau_0 = 0.2$ fm, and the EoS is the $s83z_{18}$ parametrization from Ref. [18].

IP-Glasma

IP-Glasma model [19, 20] is based on Color Glass Condensate [21–24]. It calculates the initial state as a collision of two color glass condensates and evolves the generated fluctuating gluon fields by solving classical Yang-Mills equations. The calculated event-by-event fluctuating initial states [25] were further evolved [26] using the MUSIC code [27–29] constrained to boost-invariant expansion. We subsequently averaged the evaluated temperature profiles to obtain one average profile per centrality class. In these calculations, the switch from Yang-Mills to fluid-dynamical evolution took place at $\tau_{\text{switch}} = 0.4$ fm, shear viscosity over entropy density ratio was constant $\eta/s = 0.12$, and the temperature-dependent bulk viscosity coefficient over entropy density ratio had its maximum value $\zeta/s = 0.13$. The equation of state was based on the HotQCD lattice results [30] as presented in Ref. [31].

T$_{\mathrm{R}}$ENTo [32] is a phenomenological model capable of interpolating between wounded nucleon and binary collision scaling, and with a proper parameter value, of mimicking the EKRT and IP-Glasma initial states. As with the EKRT initialization, we create an ensemble of event-by-event fluctuating initial states, sort them into centrality classes, average, and evolve these average initial states. Unlike in other cases, we employ the version of the VISH2+1 code [33] described in Refs. [34, 35]. We run the code using the favored values of the Bayesian analysis of Ref. [35]; in particular, allow free streaming until $\tau = 1.16$ fm, the minimum value of the temperature-dependent η/s is 0.081, and the maximum value of the bulk viscosity coefficient ζ/s is 0.052. The EoS is the same HotQCD lattice results [30] based parametrization as used in Refs. [34, 35].